Available online at www.sciencedirect.com
ScienceDirect
Continental Shelf Research 27 (2007) 613–633
CONTINENTAL SHELF RESEARCH
www.elsevier.com/locate/csr

Sediment transport and resuspension due to combined motion of wave and current in the northern Adriatic Sea during a Bora event in January 2001: A numerical modelling study

X.H. Wang[a,*], N. Pinardi[b], V. Malacic[c]

[a]*School of Physical, Environmental and Mathematical Sciences, University of New South Wales at Australian Defence Force Academy, Canberra, ACT 2600, Australia*
[b]*Corso di Scienze Ambientali, University of Bologna, Ravenna, Italy*
[c]*National Institute of Biology, Piran, Slovenia*

Received 15 November 2005; received in revised form 4 October 2006; accepted 12 October 2006
Available online 5 January 2007

Abstract

The Adriatic Sea general circulation model coupled to a third generation wave model SWAN and a sediment transport model was implemented in the Adriatic Sea to study the dynamics of the sediment transport and resuspension in the northern Adriatic Sea (NAS) during the Bora event in January 2001. The bottom boundary layer (BBL) was resolved by the coupled model with high vertical resolution, and the mechanism of the wave–current interaction in the BBL was also represented in the model. The study found that, during the Bora event of 13–17 January 2001, large waves with significant wave height 2 m and period of 5 s were generated by strong winds in the northwestern shelf of the Adriatic where the direction of wave propagation was orthogonal to the current. The combined motion of the wave and current in the BBL increased the bottom stress over the western Adriatic shelf, resulting in stronger sediment resuspension there. Combining stronger bottom resuspension and strong upward vertical flux of resuspended sediments due to turbulent mixing, the model predicted that sediment concentration near the Po River was much higher than that predicted by the model run without wave forcing. The study also shows that wave–current interaction in the BBL reduced the western Adriatic Coastal Currents (WACCs) in the shallower north. It is concluded that wave forcing significantly changed the sediment distributions and increased the total horizontal fluxes over the western shelf. These results signified wave effect on sediment flux and distribution in the NAS, and suggested that waves cannot be neglected in the study of dynamics of sediment transport and resuspension in the shallow coastal seas. By including the tidal forcing in the coupled model, we also examined the effect of tides on the sediment transport dynamics in the NAS.

Keywords: Sediment transport and resuspension; Adriatic sea; Wave–current interaction; Tides; Sediment transport; Benthic boundary layer; Numerical modelling

1. Introduction

The Adriatic Sea is a semi-enclosed shelf sea located between western and eastern parts of the Mediterranean Sea. The basin has an elongated

*Corresponding author. Tel.: 61 2 62688473; fax: 61 2 62688786.
E-mail address: hua.wang@adfa.edu.au (X.H. Wang).

0278-4343/$ - see front matter © 2006 Elsevier Ltd. All rights reserved.
doi:10.1016/j.csr.2006.10.008

shape approximately 800 km long and 200 km wide with an area of 160,000 km^2. It consists of a shallow northern shelf, arriving at 45°N, a depression of 270 m in the middle basin (Jabuka Pit), and a deep southern part with a maximum depth of 1320 m. On the western coast of the Adriatic Sea, the shelf has a gradual slope with isobaths running parallel to the coastline. The eastern coast is irregular, and composed of many islands with steeper continental shelf breaks. Our study will be focused in the shallow northern shelf and the middle basin defined as the northern Adriatic Sea (NAS, Fig. 1).

The Po River is the main source of freshwater in the Adriatic, providing up to 50% of total river runoffs. The Po River discharges at an annual average rate of 1500 m^3 s^{-1}, with two peaks during spring and autumn. The meteoclimatology of the area presents strong northeasterly winds during winter, called Bora, while during summer and autumn winds could be southeasterly with smaller amplitude (Scirocco). On the western Adriatic coast, Bora is a downwelling favourable wind and can generate large waves with significant wave heights of 1 m, and period of 5 s (Cavaleri et al., 1997). In contrast, Scirocco is an upwelling favourable wind which generates lower wave height, but longer wave period in order of 10 s in the NAS region.

The general circulation of the Adriatic Sea is cyclonic and highly variable with seasons (Artegiani et al., 1997a, 1997b; Malanotte-Rizzoli and Bergamasco, 1983; Zavatarelli et al., 2002; Zavatarelli and Pinardi, 2003; Pullen et al., 2003). One of the major features is a coastal current along the western side of the basin, the Western Adriatic Coastal Current (WACC), driven by wind and thermohaline forcing. The WACC reaches maximum amplitude during winter due to the strong Bora wind energy input but persists throughout the year, breaking into several baroclinic jets during the other seasons (Poulain, 2001). The thermohaline structure of the WACC is connected to the Po River fresh water river runoff and winter surface heat loss in the NAS (Raicich, 1996; Kourafalou, 1999; Wang, 2005).

Tidal dynamics in the Adriatic Sea has been studied by a number of authors (e.g. Malacic et al., 2000). Tides are relatively weak in the Adriatic Sea dominated by M_2 with amplitude less than 0.3 m in the Port of Trieste. In the northern end of the Adriatic the tidal range is approximately 1 m, causing a tidal current about 0.1 m s^{-1}. Malacic et al. (2000) used a two-dimensional finite difference model with very high horizontal resolution to simulate the tides in the NAS. They found that the semidiurnal tides in the NAS can be represented by a system of incoming and reflected Kelvin waves, whose amplitudes reach maximum along the coast, and decrease rapidly towards the centre of the basin. In contrast, diurnal tides are topographic waves propagating from the east to the west coast, and the amplitudes are rising from the South to the North.

In the NAS, two main classes of sediments can be identified (Brambati et al., 1973). The first class consists of coarser sediments of sand with grain size between 50 and 2000 μm. The second class is of finer materials of silt with grain size between 2 and 50 μm. It has long been recognized that the fine sediments such as fine sand, silt and clay are mainly supplied from the NAS rivers, and transported southward by the coastal current (e.g. Brambati et al., 1973; Ravaioli et al., 2003; Sherwood et al., 2004; Nittrouer et al., 2004). Thus, it is known that the depocentres in NAS are located south further away from the Po River mouths with thickest portions at Ancona and Gargano Peninsula (Fig. 1a, Correggiari et al., 2001). Flocculation of the fine sediments also occurs and is mainly found in these rivers and estuaries before they reach the ocean. However, the bulk of floc deposition occurred immediately offshore of the main distributaries of the Po River with a water depth less than 10 m (Nittrouer et al., 2004; Fox et al., 2004a; Mikkelsen et al., 2005). Fox et al. (2004b) applied three different methods including Stokes' approximation to assess the relationship between aggregate size and settling velocity. All methods conformed to the finding of the floc settling rate of 10^{-3} m s^{-1} in the waters adjacent to the Po River mouth.

Recently, based on a wave–current interaction model with idealized wave fields, Wang and Pinardi (2002) argue that wave-driven sediment resuspension is an important resuspension mechanism in the shallow coastal areas of the NAS, and contributes significantly to the complexity of the sediment distribution and flux features in the region. Their results were able to show the difference in sediment deposition/resuspension between fine and coarse sediments and their fluxes in the northern basin. However, the computations were idealized and waves were assumed to be constant in amplitude and direction in the basin. Furthermore, the effect of tides on the sediment transport and resuspension was not considered.

Since the modelling study of Wang and Pinardi (2002), several major international research

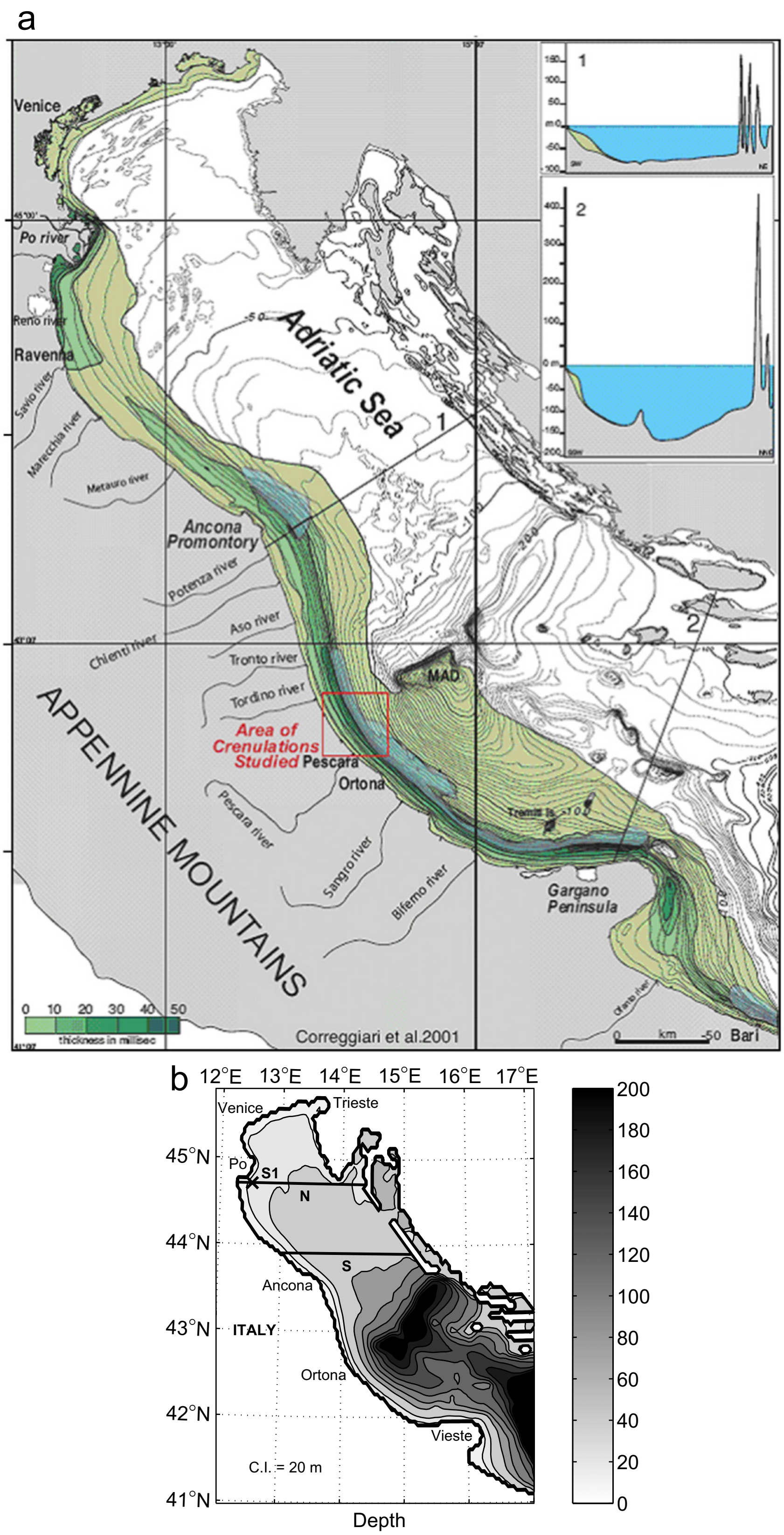

Fig. 1. (a) The northern Adriatic Sea bathymetry and Holocene sediment depositions. Figure from Correggiari et al. (2001); (b) the NAS model domain. S1 denotes location for station S1. N and S denote two cross-sections south of the Po River delta, and near Ancona, respectively.

programmes have been implemented in the Adriatic Sea, with a focus of atmospheric forcing and oceanic responses and sediment transport dynamics. EuroStrataform is one of such programmes designed to study sedimentation and mass transport in the NAS. Reviews of EuroStrataform project are provided by Sherwood et al. (2004) and Nittrouer et al. (2004). Some of major conclusions of these studies can be summarized in the following.

Observations of sediment dynamics on the Po prodelta have shown that wave-driven turbidity flows occurred during the periods of high waves (e.g. during Scirocco events, Traykovski et al., 2006). These flows are confined to the wave bottom boundary layers (BBLs) and play a major role in cross-shore sediment transport, although along-shore transport of the sediments were an order of magnitude larger due to wind forced mean currents during the winter Bora events.

During Po River floods such as the event in 2000, the direct fallout due to flocculation from the surface plume forms the dominant mechanism for sediment delivery to the seabed near the Po delta (Wheatcroft et al., 2006). Further offshore at the depth of 15–20 m, a persistent benthic nepheloid layer was also detected with a load in order of $50\,\mathrm{g\,m}^3$, probably suspended from the seabed (Boldrin et al., 2005). However due to its relatively low sediment concentration, the turbidity generated density current is less likely to be formed, although Khan et al. (2005) predicted that hyperpycnal plumes may have occurred in the northern Adriatic rivers during these floods. Finally, Palinkas et al. (2005) used the penetration depths of short-lived radioisotope ^{7}Be (half-time 53 d) and ^{234}Th (half-time 24 d) to estimate seasonal deposition rates of sediments, and found that the maximum rates ranged from 2 to $6\,\mathrm{cm\,yr}^{-1}$ in the Po River mouth dispersal system.

This paper uses an Adriatic Sea general circulation model (Adriatic intermediate model, AIM) coupled to a sediment transport model and a third generation wave model (Simulating waves near-shore, SWAN) in order to study the dynamics of sediment transport and resuspension due to combined motion of current and wave in the BBL in the NAS. We considered a wave–current interaction in the modelling of the BBL dynamics in order to examine the wave effect on the bottom stress and sediment resuspension. A particular focus of this work is to combine realistically simulated current and wave fields to examine sediment flux and distribution features in the NAS during the Bora event of 13–17 January, 2001. This allows us to address two major issues that have not been studied in past, namely (1) effect of waves (including the effect of wave–current alignment) on sediment resuspension and transport in NAS using realistic wave fields; (2) effect of tides on sediment transport in the NAS. The next section describes the general circulation model (AIM), the wave model (SWAN), the sediment transport model, and the parameterization for the bottom stress under wave–current interaction in the BBL. Model results are discussed in Sections 3, and a final section offers discussion and conclusions.

2. Model description

2.1. Adriatic intermediate model

The AIM is based on the three-dimensional Princeton Ocean Model (POM) (Blumberg and Mellor, 1987) which uses a seabed following sigma coordinate system, and proves to be advantageous in the study of the BBL dynamics (e.g. Mellor and Wang, 1996; Wang, 2002; Byun and Wang, 2005). The AIM was implemented in the whole Adriatic Sea with a regularly spaced grid of 5 km (Zavatarelli and Pinardi, 2003). The model time steps were 7 and 700 s for external and internal modes, respectively. The model had 21 sigma coordinate levels that were distributed logarithmically in the bottom and surface boundary layers to increase resolution there. In the shallow northern Adriatic and along the western shelf areas, the BBL was resolved by a set of levels less than a meter thick above the seabed. The model used the conventional 2.5 Mellor–Yamada turbulence closure submodel and the Smagorinsky horizontal viscosity parameterization (Smagorinsky, 1963). A detailed description of the model can be found in Zavatarelli and Pinardi (2003).

2.2. Wave model

A third generation wave model SWAN was implemented in the Adriatic Sea. SWAN was developed to simulate the wave parameters for shallow coastal waters at Delft University Technology. The model is based on the two-dimensional wave action balance equation including energy density generation and dissipation terms by wind, white-capping, depth-induced wave breaking, bottom friction and redistribution of wave energy due to wave–wave interaction. The propagation in geographical space, the shifting of the relative frequency due to variation in depth, refraction due to bottom and current variations are also taken into account by the model. For a detailed description of the SWAN model, refer to Holthuijsen et al. (1989), Booij et al. (1999) and Ris et al. (1999).

In this paper, we used SWAN in stationary mode to compute the Adriatic Sea wave fields under forcing of 6-h ECMWF analysis wind. The depth-induced wave breaking was enabled with default options and parameters. The bottom friction was computed by the Madsen scheme with default equivalent bottom roughness length scale. The model had 18 uniformly distributed directions, and the frequency resolution was determined by $f_{i+1} = 1.9f_i$ with $f_{max} = 1.0\,\mathrm{Hz}$ and $f_{min} = 0.04\,\mathrm{Hz}$. The model domain had a uniform spatial grid of 5 km. Incoming waves at the southern open boundary was assumed to be zero.

2.3. The effect of the wave–current interaction on the bottom stress

When waves were not considered in the BBL, the bottom stress τ_b is due to the near bottom mean currents and expressed as

$$\tau_b = \rho C_d |u_b| u_b \tag{1a}$$

and

$$C_d = \mathrm{Max}\left\{ \left[\frac{1}{\kappa} \ln(H + z_b)/z_0 \right]^{-2}, 0.0025 \right\}. \tag{1b}$$

Here κ is the von Karman constant, H is the total water depth, z_o is the bottom roughness and $\boldsymbol{u}_b$ is the mean current velocity field at the model bottom level ($z = z_b$). This parameterization would be changed and z_o would be modified if the effect of wave–current interaction on the bottom stress was considered according to Grant and Madsen (1979).

Based on the analytical theory by Grant and Madsen (1979), the maximum bottom stress $|\tau_{bmax}|$ due to the combined motion of waves and current in the BBL can be computed by using a modified bottom stress quadratic drag law with a wave–current friction factor f_{cw}:

$$|\tau_{bmax}| = \tfrac{1}{2} f_{cw} \rho (|u_b|^2 + |u_w|^2 + 2|u_b||u_w| \cos\theta), \tag{2}$$

where u_w is the bottom wave orbital velocity calculated by the SWAN simulated characteristic equivalent wave fields (Madsen et al., 1988), θ is the angle between u_b and u_w. For given waves with u_w, z_0 and f_{cw} can be computed by an iterative procedure described by Grant and Madsen (1979). In computation of Eq. (2), we had allowed the mean current u_b acted at any angle with the direction of the wave orbital velocity u_w.

Because the tides are relatively weak, we firstly excluded the tidal forcing in the model experiments by assuming the tide induced sediment transport in the NAS is insignificant in comparison with that driven by the waves and the mean current. The validity of this assumption would be examined later.

2.4. Sediment transport model

The sediment transport model was developed by Wang (2001, 2002) and Wang and Pinardi (2002). The model assumes that the resuspended sediments do not flocculate or aggregate so that they are noncohesive and the sediment mixture behaves as a Newtonian fluid. The model neglects the inertia of the sediment particles, therefore their vertical velocity differs from that of water by a small constant settling velocity w_s. Finally, we assumed that the resuspended sediment concentrations had no effect on the water density, due to relatively small sediment concentrations in the NAS. This assumption has been validated in the previous work (Wang and Pinardi, 2002), and again in this study.

The three-dimensional model describing the sediment transport dynamics in the water column is based on the advection–diffusion equation for an incompressible flow:

$$\frac{\partial C}{\partial t} + \frac{\partial}{\partial x}(uC) + \frac{\partial}{\partial y}(vC) + \frac{\partial}{\partial z}[(w + w_s)C] = \frac{\partial}{\partial z}\left(K_h \frac{\partial C}{\partial z} \right) + F_C, \tag{3}$$

where x, y, z, u, v, w represent zonal, meridional and vertical (positive upward) coordinates and their velocity projections, C is the sediment concentration ($\mathrm{g\,m^{-3}}$), K_h is the vertical eddy diffusivity coefficient equal to that of heat and salt, F_C is the horizontal diffusion term for C. The advection term is differenced according to the three-iteration Smolarkiewicz upstream scheme (Smorlarkiewicz, 1984).

We used two sets of equations like Eq. (3) concomitantly in the model: one for the coarse sediment material (CSM) and the second for the fine sediment material (FSM).

2.4.1. Model boundary condition

Seventy percent of the lateral sediment flux from all Adriatic Sea rivers, totalling 1.67 Mt per month (Frascari et al., 1988), was distributed at the Po River mouth. The rest was equally distributed at the other rivers or land drainage areas along the Adriatic coast. Brambati et al. (1973) observed that the areal distribution of the coarse materials (sand) over the Italian coast strip can reach highest percentage of 50%. For simplicity, we assumed that the sediment discharges from river sources carried an equal load of the CSM and the FSM components. At the southern open boundary incoming FSM and CSM concentration was assumed to be zero.

The bottom sediment flux was prescribed according to

$$K_h \frac{\partial C}{\partial z} - w_s C = S \text{ at } z = -H \tag{4}$$

where according to Ariathurai and Krone (1976), the seabed sediment flux S due to deposition or resuspention can be formulated in the following:

$$S = \begin{cases} S_0\left(1 - \frac{|\tau_b|}{\tau_c}\right) \text{if} |\tau_b| > \tau_c, \\ C_b w_s\left(\frac{|\tau_b|}{\tau_c} - 1\right) \text{if} |\tau_b| < \tau_c. \end{cases} \tag{5}$$

Here S_0 is an empirical constant and was set to $10^{-4}\,\mathrm{kg\,m^{-2}\,s^{-1}}$ (Clarke and Elliott, 1998); τ_c is the critical stress for erosion and deposition and was set to $0.02\,\mathrm{N\,m^{-2}}$ according to Shields function with a sediment density $\rho_s = 1100\,\mathrm{kg\,m^{-3}}$ for sediments such as fine sand and silt ($20 < d < 60\,\mu\mathrm{m}$), Stokes law yields the settling velocity w_s from -1×10^{-4} to $-1\times10^{-5}\,\mathrm{m\,s^{-1}}$, thus w_s was chosen to be -10^{-5} and $-10^{-4}\,\mathrm{m\,s^{-1}}$ for FSM and CSM, respectively; and C_b is the suspended sediment concentration at the model bottom layer. Bottom stress τ_b was computed by (1) for the model run without waves; or by (2) with waves. A detailed discussion on the choice of the model parameters was given by Wang and Pinardi (2002). Admittedly, above assumptions such as a uniform bed erodability are simplifying ones that have potential impact on predicting the actual sediment transport rates in the NAS as pointed out by a reviewer. The most important thing here is to build a model with reasonable approximation of sediment processes that can be used to quantitatively study the ways and extent to which an observed Bora storm event can affect these processes in the study region.

It should be noted here that since the flocculation of FSM is mainly found near the Po River mouth before they reach the ocean (Nittrouer et al., 2004; Fox et al., 2004b), with the bulk of floc deposition occurring in the water depth less than 8 m (Fox et al., 2004a), the model sensitivity to a larger settling velocity of suspended sediments in order of $-10^{-3}\,\mathrm{m\,s^{-1}}$ as used by Sherwood et al. (2004) was also tested in this study.

3. Model results

The AIM was run with realistic wind stress, surface heat flux, and river runoff forcings continuously from 1 January 1999 to 31 January 2001. As initial condition the fields from the climatological simulation of the Adriatic Sea circulation (Zavatarelli and Pinardi, 2003) were used. The sediment transport model was coupled to the AIM from 1 December, 2000. Two benchmark numerical experiments were conducted first in order to investigate sediment transport and resuspension due to wave–current interaction. In Experiment 1, the wave effect on the bottom stress was not considered. In Experiment 2, the SWAN simulated

Table 1
Model predicted FSM and CSM southward sediment flux at the cross sections N and S on day 15

	SWAN wave forcing	Tide forcing	$\rho = \rho(C)$	Cross section N ($\mathrm{kg\,s^{-1}}$)		Cross section S ($\mathrm{kg\,s^{-1}}$)	
				FSM	CSM	FSM	CSM
Expt. 1	No	No	No	10,542	9343	7149	4294
Expt. 2	Yes	No	No	25,565	24,104	10,738	7890
Expt. 3	Yes[a]	No	No	27,703	26,214	10,742	7910
Expt. 4	Yes	Yes	No	25,348	23,697	8631	6169
Expt. 5	Yes	No	Yes	25,529	24,080	10,845	7940

'No' indicates an exclusion of the forcing function in the model experiment.
[a]Experiment 3 assumed that the waves and bottom currents are aligned.

wave fields were used for wave–current interaction in the BBL from 1 January 2001. Effects of wave and current alignment, tides and sediment-induced stratification on the NAS sediment transport were examined later in Experiments 3, 4 and 5, respectively (Table 1).

January 2001 was a typical month for the winter meteoclimatology when a strong Bora event was identified from 13–17 January. Fig. 2a shows the wind stress and net surface heat flux computed at Station S1 (Fig. 1), using the ECMWF 6-h analysis data in January 2001, and the bulk aerodynamic formulae as in Maggiore et al. (1998). The wind stress vectors were on the conventional geographical coordinate system. The Bora event was caused by a low-pressure system located on southern Italy, advecting air from Eurasia with wind stress up to $1\,\mathrm{N\,m^{-2}}$ in the NAS, and causing the maximum net surface heat loss of $800\,\mathrm{W\,m^{-2}}$ over the north-eastern shelf on 15 January (Fig. 2b). Under such strong wind and surface cooling forcing conditions, and with realistically simulated wave fields, we have a particular interest in examining the wave effect on the sediment dynamics in the NAS.

3.1. Current and wave fields during the Bora event

The AIM simulated surface and bottom currents in the NAS during the Bora event on 15 January are shown in Fig. 3a. The Bora wind generated barotropic onshore currents that connected to and strengthened the partially buoyancy driven WACC. The maximum currents reached $1.3\,\mathrm{m\,s^{-1}}$ near the Po mouth at the surface and $0.3\,\mathrm{m\,s^{-1}}$ at the bottom near Ortona.

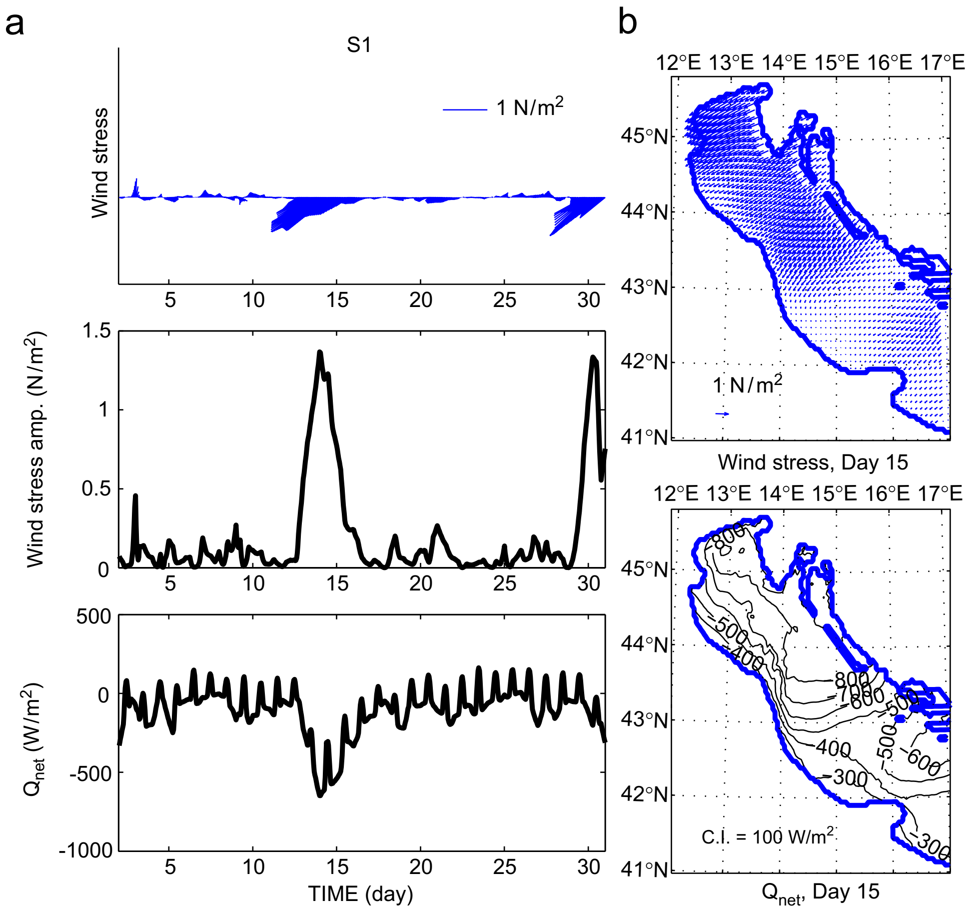

Fig. 2. (a) January 2001 wind stress and net surface heat flux at station S1. The European Centre for Medium Range Weather Forecast (ECMWF) 6-h analysis wind fields were used for the wind stress computation. The wind stress vectors were on the conventional geographical coordinate system. The ECMWF and COADS (Comprehensive Ocean Atmosphere Data Set) data were used to compute the surface heat flux with the bulk aerodynamic formulae. (b) ECMWF wind stress and net surface heat flux over the northern Adriatic Sea on 15 January 2001.

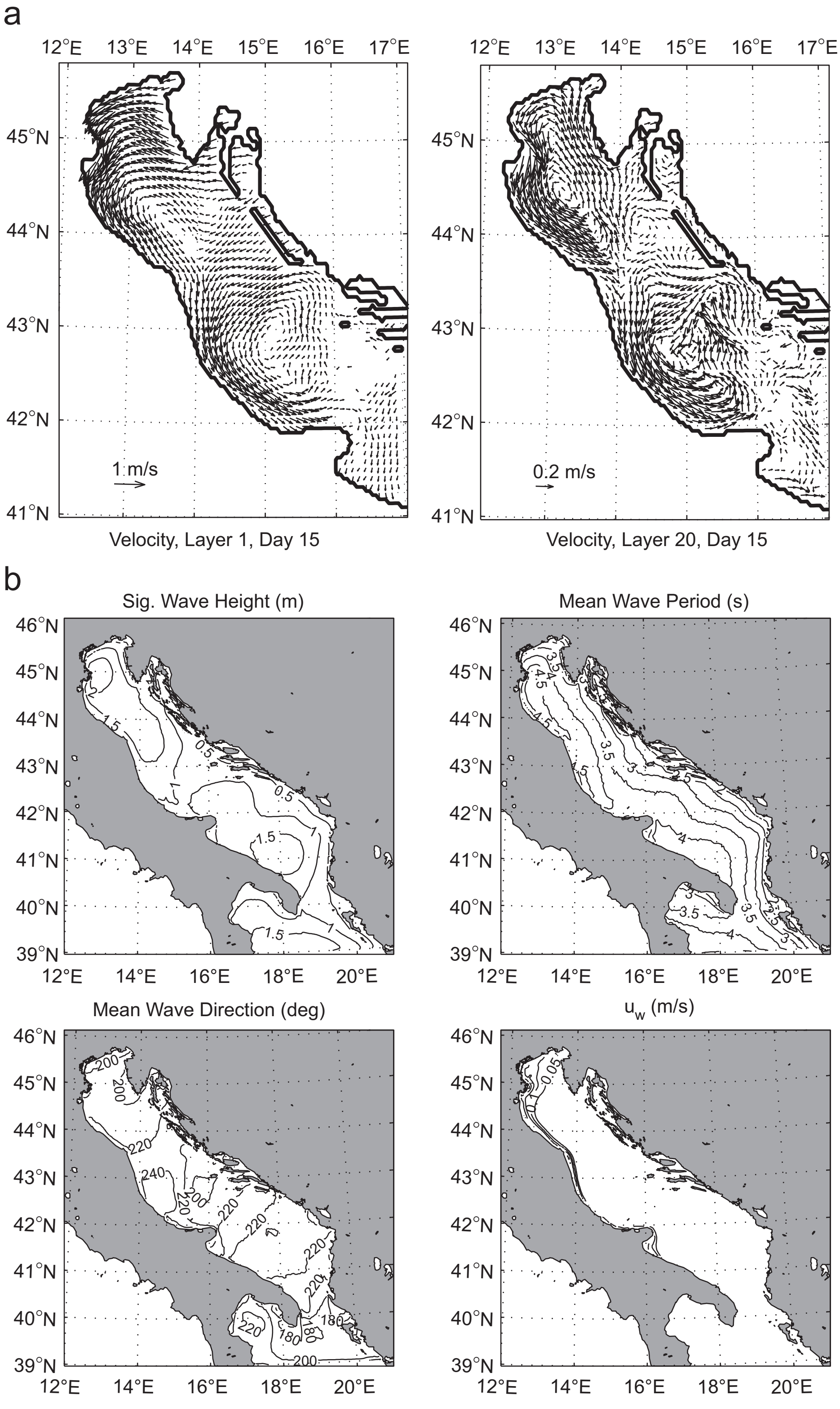

Fig. 3. (a) Model predicted surface (layer 1) and (c) bottom (layer 20) velocity fields on 15 January 2001. Vectors less than 10% of maximum velocity are not plotted. (b) SWAN predicted significant wave height, mean wave period, mean wave direction and wave bottom orbital velocity for entire Adriatic Sea on 15 January 2001.

The bottom WACC was largely bottom steered and parallel to the isobaths along the western Adriatic coast. These general features of the coastal current agreed with the observations by Lee et al. (2005) along the western Adriatic coast, although the coarse ECMWF wind fields may have failed to capture the smaller-scale interior vorticity due to orographic incisions in the Dinaric Alps (e.g. Pullen et al., 2003). Since the WACC is the current important to the NAS sediment fluxes over the western shelf, this agreement provided the realistic physical background and fields for modelling sediment transport dynamics in the NAS during the Bora event.

On the same day, the SWAN predicted significant wave height, mean period, mean direction and wave bottom orbital velocity for the entire Adriatic Sea (Fig. 3b). Maximum wave height and period was predicted at the mouth of Po with 2 m and 4.5 s, respectively, resulting in a maximum bottom wave orbital velocity of 0.2 m s^{-1}. It should be noted, that as the Bora wind was an onshore wind, the waves there were fetch-limited and purely generative. Therefore, the Bora wave fields had larger cross-shore gradients, with higher wave heights and periods on the west coast, than on the east coast. Furthermore, the mean wave direction was aligned with the wind direction, and tended to be perpendicular to the coastline along the western Adriatic coast due to wave refraction, therefore orthogonal to the bottom currents there.

The model prediction of the wave fields was validated by the wave data observed by the wave buoys at Ancona (43°37.00′N, 13°51.00′E) and Ortona (42°24.07′N, 14°32.04′E) at 3-h intervals (Fig. 4). Good agreement was achieved for waves under low to moderate wind conditions at both platforms. For higher wind conditions such as Bora events, the model predicted wave height was comparable with that of the observation at Ortona. However, the wave response at Ancona was underestimated by up to 50%. This was caused by the global scale ECMWF wind fields that has a practical horizontal resolution of 40 km, incapable of resolving fine scale wind variability in the NAS due to the complex orography there (Cavaleri and Bertotti, 1997; Signell et al., 2005).

3.2. Effect of waves on BBL hydrodynamics and sediment resuspension

The effect of waves on BBL hydrodynamics and sediment resuspension will be examined at station

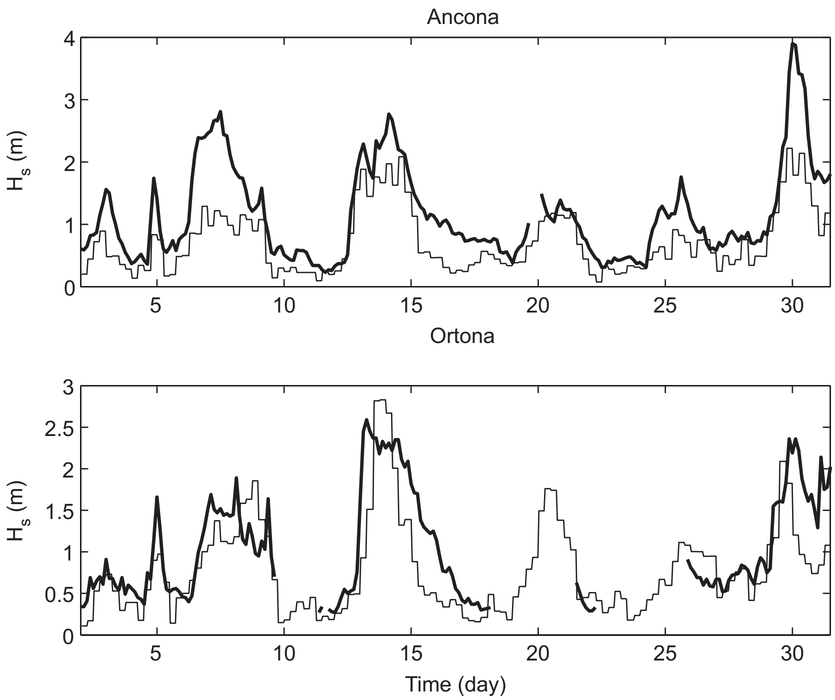

Fig. 4. Comparison of hourly significant wave height predicted by SWAN (thin line) and 3-h measurements (thick line) at Ancona (43°37.00′N, 13°51.00′E) and Ortona (42°24.07′N, 14°32.04′E).

S1. Station S1 is located at a water depth of 20 m adjacent to Po River delta, and is a subject of several recent field studies reported in the literatures (e.g., Matteucci and Frascari, 1997; Boldrin et al., 2005; Trakovski et al., 2006). When the wave effect was not considered (Expt. 1 in Fig. 5), the current speed at the bottom reached a maximum of $0.34\,\mathrm{m\,s^{-1}}$ during the Bora event of 13–17 January. The Bora event increased the bottom stress to $0.66\,\mathrm{N\,m^{-2}}$ from a background value of about $0.01\,\mathrm{N\,m^{-2}}$. The increase in the bottom stress resulted in the bed load erosion, initially causing a noticeable increase in FSM and CSM concentrations at the bottom, and then a well mixed water column from 13–17 January. During the periods when the resuspension was weak, the FSM sediment concentration at the surface was larger than that at the bottom, and was dominantly controlled by the

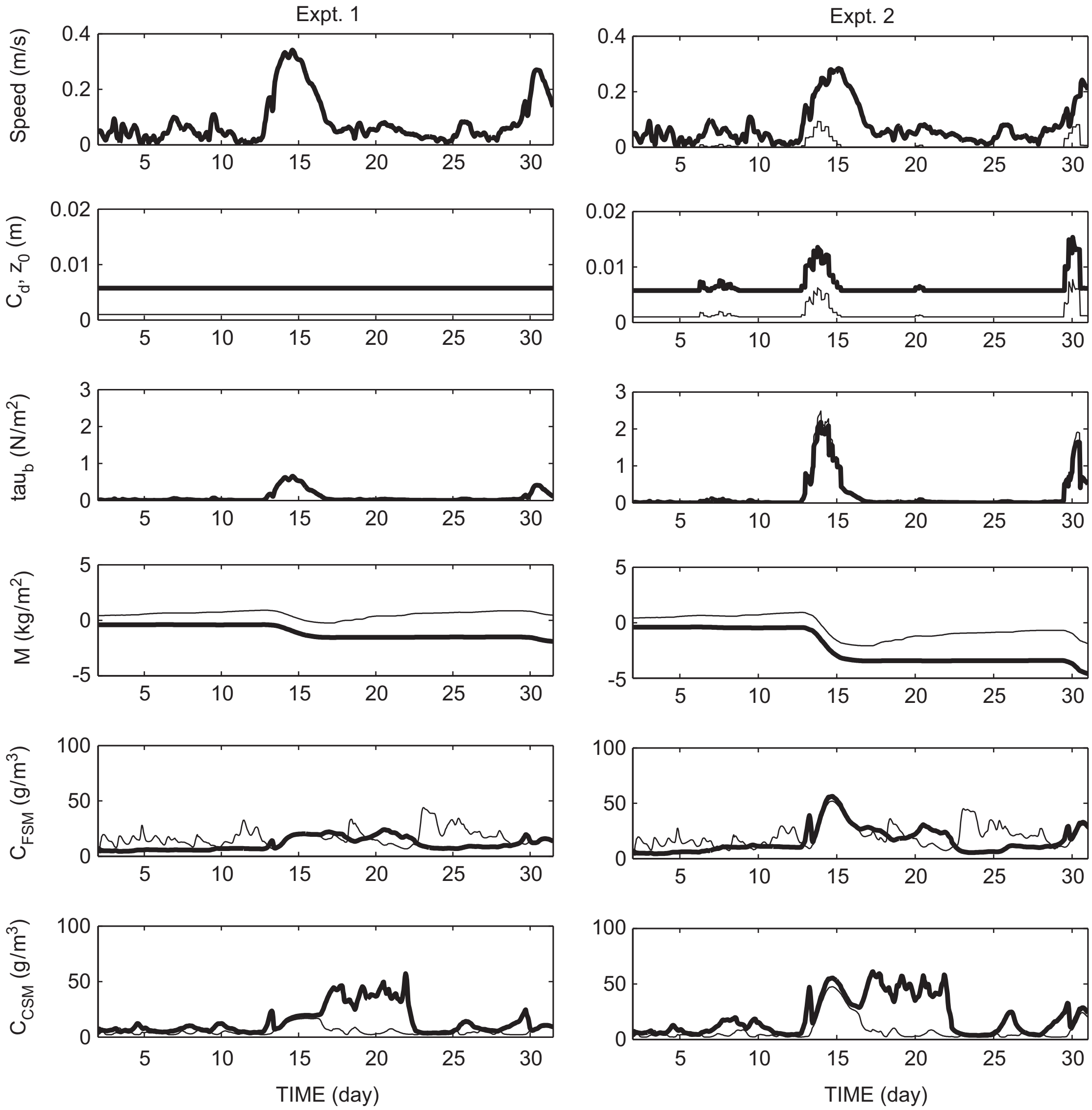

Fig. 5. The hourly time series of BBL hydrodynamics properties, bed load, and sediment concentrations in January 2001 at station S1 predicted by Experiment 1 (left) and Experiment 2 (right). From top: the bottom mean current (thick line) and bottom wave orbital velocity (thin line); the bottom roughness z_0 (thin line) and drag coefficient C_d (thick line); bottom stress τ_b predicted by Experiments 1 and 2 (thick line) and Experiment 3 (thin line); sedimentation (bed load M) for FSM (thick line) and CSM (thin line); FSM concentration C_{fsm} at surface (thin line) and bottom (thick line); CSM concentration C_{csm} at surface (thin line) and bottom (thick line). Bed load is the time integration of the bottom sediment flux due to deposition and resuspension.

sediment discharge from the Po River. The large bottom CSM concentration between 17 and 22 January were produced by the sediment settling.

When the wave effect was considered (Expt. 2 in Fig. 5), the large waves during the Bora event increased the bottom roughness z_0 from 0.001 m to a maximum of 0.008 m. This in turn increased the bottom drag coefficient C_d from 0.0048 to a maximum value of 0.015 and the maximum bottom stress during the Bora was $2.2\,\mathrm{N\,m^{-2}}$, a value that is three times larger than that simulated by Experiment 1. In response to the wave enhanced bottom stress, the FSM and CSM concentration was 80% higher than that predicted by the model run without wave forcing. As expected, the maximum mean current at the bottom was also reduced by 18% compared with Experiment 1, and reached $0.28\,\mathrm{m\,s^{-1}}$. The maximum bottom wave orbital velocity was $0.09\,\mathrm{m\,s^{-1}}$.

Fig. 6a shows the bottom stress on 15 January predicted by Experiment 1. High bottom stress was predicted in the northern shelf and along the Italian coast, where the bottom currents were strong. Consequently, large sediment concentration was observed on the western Adriatic shelf with maximum surface concentration reaching $28\,\mathrm{g\,m^{-3}}$ near the Po River delta (Fig. 7a). Since the CSM concentration was very similar to that of FSM and there was negligible vertical variation in the sediment concentration north of Vieste, only the surface FSM field is shown.

Figs. 6b and 7b show the bottom stress and surface FSM field simulated by Experiment 2 that included the effects of wave–current interaction in the BBL. Although the distribution patterns were similar to those of Experiment 1, both bottom stress and sediment concentration exhibited increase in their magnitudes by a maximum value of $1.3\,\mathrm{N\,m^{-2}}$ and $50\,\mathrm{g\,m^{-3}}$, respectively, in the nearshore region from Po River to Ancona (Figs. 6c and 7c). The mismatch between two locations of maximum differences in the bottom stress and surface sediment concentration was caused by the WACC

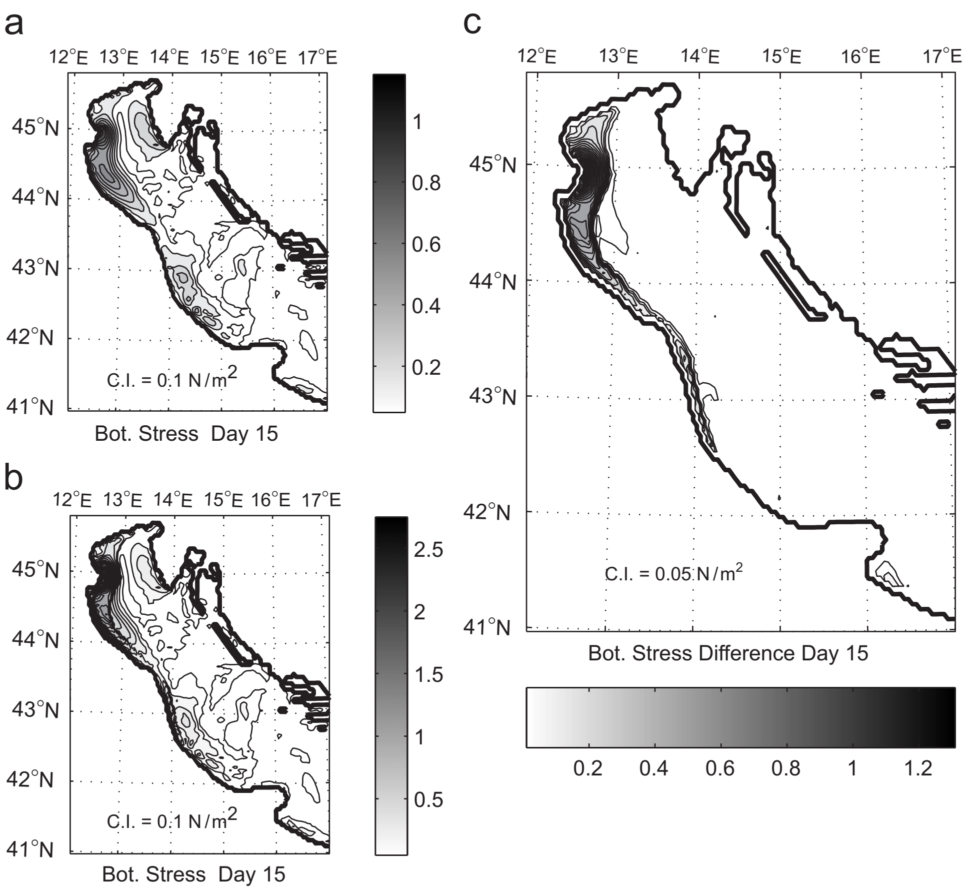

Fig. 6. The bottom stress on 15 January 2001, predicted by Experiment 1 (a), Experiment 2 (b), and their difference (c).

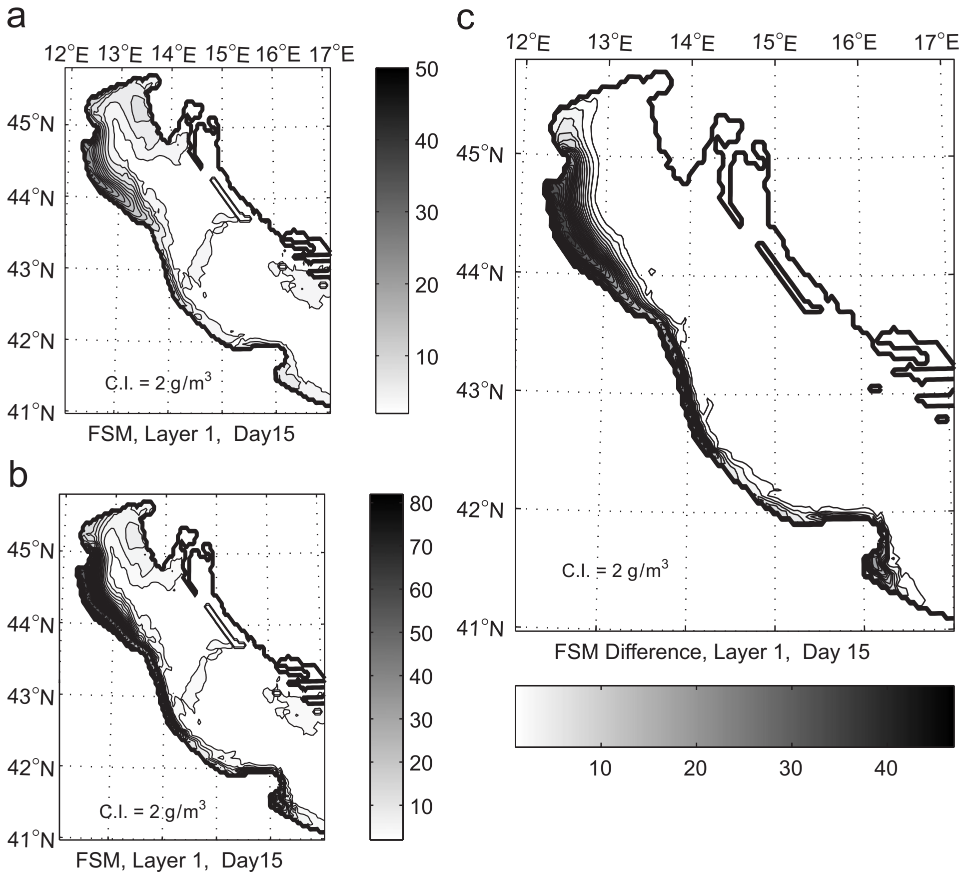

Fig. 7. The surface (layer 1) FSM concentration on 15 January 2001, predicted by experiment 1 (a), Experiment 2 (b), and their difference (c).

southward advection of suspended sediments. We note that these increase only occurred during and immediately after the Bora event when the waves with height and period more than 1.5 m and 4.5 s were simulated on 15 January. We also noted that the FSM concentration simulated by Experiment 2 is in good agreement with Boldrin et al. (2005) who found the maximum suspended sediment concentration near Po River is $45\,\mathrm{g\,m^{-3}}$ for January 2001 as shown in Table 2. During a Bora event in January 2003 that had similar wave and current forcing conditions, Trakovski et al. (2006) also observed a sediment concentration in a range of $70–100\,\mathrm{g\,m^{-3}}$ at 1 mab (Table 2).

3.3. *Effect of waves on southward sediment flux*

During the Bora event on 15 January, the vertical mixing was vigorous in the water column, and produced a net upward sediment flux despite downwelling currents observed along the Italian coast (Fig. 8). The high turbulence intensity was primarily produced by the strong current shear. The surface cooling further intensified the vertical mixing. The model predicted vertical eddy diffusivity at cross section N ranged from $0.02\,\mathrm{m^2\,s^{-1}}$ on the western coast to $0.12\,\mathrm{m^2\,s^{-1}}$ near the centre of the basin, and its maximum value was two times larger than that before the Bora event on 10 January (Fig. 9). We note that due to the shallow water depth in the NAS, both surface and bottom boundary layers occupied the entire water column thus the mixing was the strongest at the mid-depth during the Bora event as shown in Fig. 9. Moreover, according to Eidsvik (1993) the wave contribution of the turbulence production above the wave boundary layer is negligible as the wave orbital velocity shear is small there. Therefore the waves have no effect on vertical eddy diffusivity in the water column as predicted by the Experiment 2.

Table 2
Model data comparison of sediment concentration, flux and sedimentation under Bora forcing conditions

Date	Forcing conditions			C (g m^{-3})	Horizontal sediment flux (g m^{-2} s^{-1})	Sedimentation rate[a] (cm yr^{-1})	Source
	Po River discharge (m^3 s^{-1})	Wave height (m)	Current speed (m s^{-1})				
Jan 01	2601	2.0	1	50	20	3.3	This study
Jan 01	2616	—	—	45	—	—	Boldrin et al. (2005)
Jan 03	2000	1.5	0.7	70–100	25	—	Traykovski et al. (2006)
Jan 01–May 03	—	—	—	—	—	2–6	Palinkas et al. (2005)

[a]An averaged bulk density value of 1500 kg m^{-3} was used in this estimate.

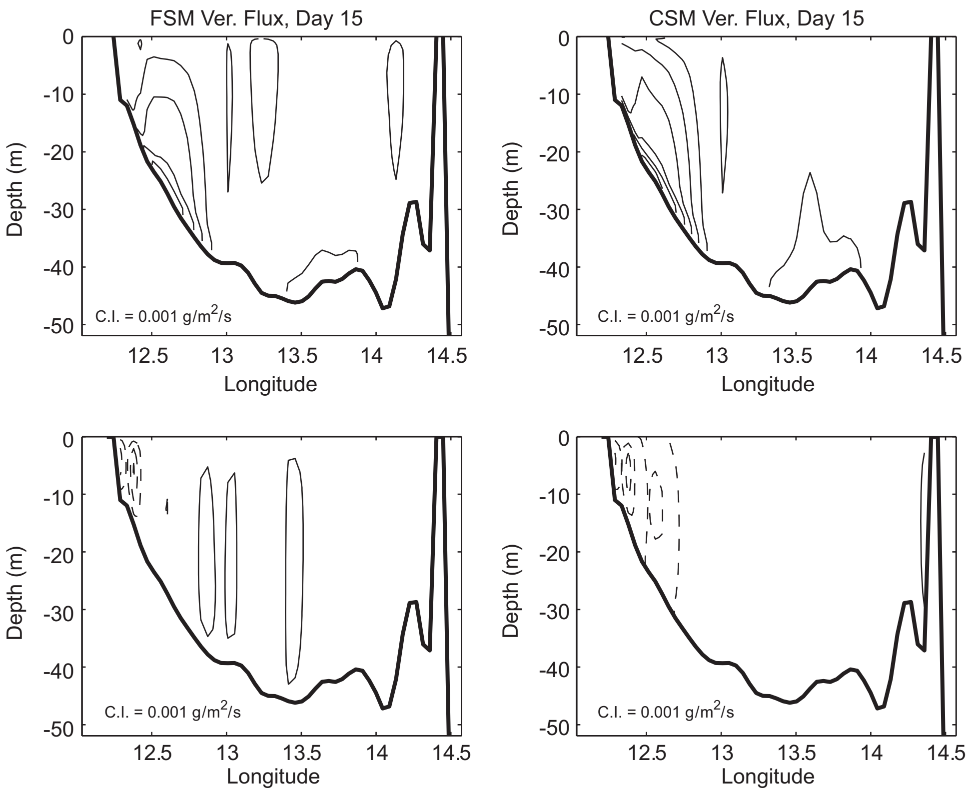

Fig. 8. Model simulated vertical FSM and CSM fluxes at cross section N on 15 January, 2001, by experiment 1. Top: $-K_h(\partial C/\partial z)$; bottom: $(w+w_s)C$. Downward fluxes are in negative values denoted by the dashed lines.

Horizontal FSM sediment flux is shown in Fig. 10, which is identical to the results of horizontal CSM flux. At the surface, wind driven onshore currents transported the sediments toward the western Adriatic coast with larger rates in a region adjacent to the Po River mouth, owing to a combination of strong currents and sediment resuspension. At the bottom, the sediment flux was southward and parallel to the coastline of the western Adriatic Sea, and was therefore able to transport the converging surface flux away from the Po delta region. The maximum sediment flux there was in order of 20 g m^{-2} s^{-1}. This prediction was compared fairly with the observed value of 25 g m^{-2} s^{-1} by Traykovski et al. (2006) in the similar forcing conditions during a Bora event in

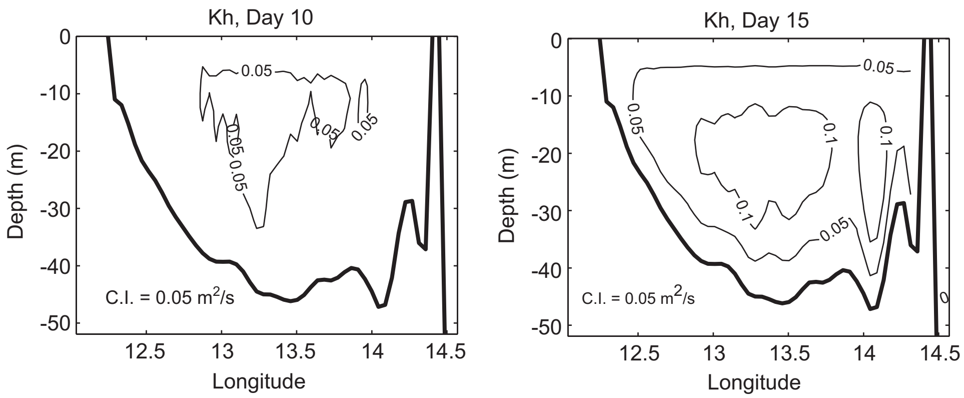

Fig. 9. Model simulated vertical eddy diffusivity at cross section N on 10 and 15 January 2001, by Experiment 1.

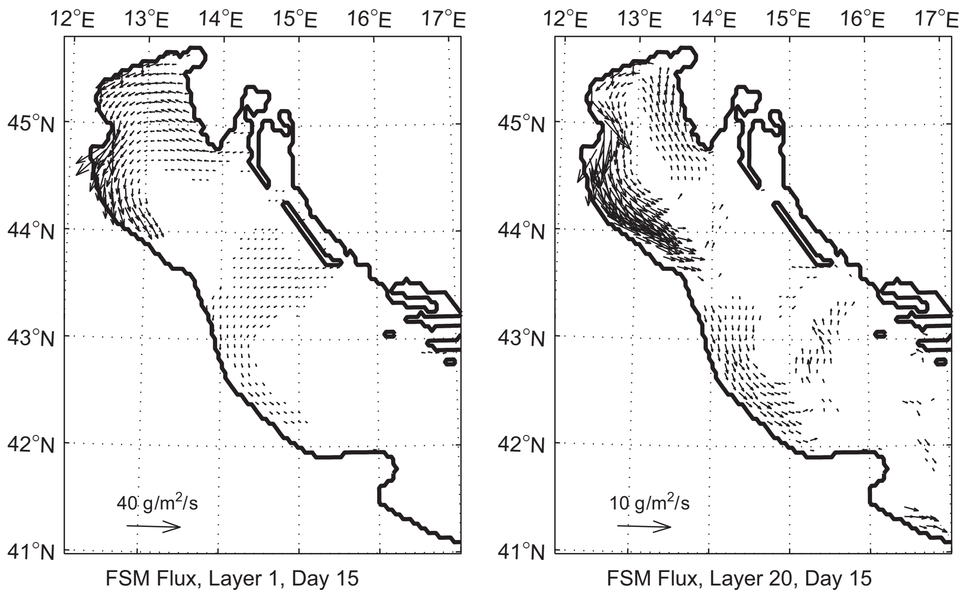

Fig. 10. Model simulated horizontal FSM fluxes at surface (layer 1) and bottom (layer 20) on 15 January 2001, by Experiment 1. Vectors less than 30% of maximum fluxes are not plotted.

January 2003 (Table 2). Note that relative strong onshore sediment flux at the surface and lack of offshore sediment flux at the bottom near Venice may be one of the mechanisms causing silting of Venice lagoon (Warren and Johnsen, 1993).

Combined with vertically well mixed sediment concentration in the water column, the Bora-enhanced WACC produced a band of southward sediment fluxes occupying the entire water column over the western shelf with depth less than 40 m (Fig. 11). The FSM and CSM flux had the same distribution pattern at the both cross sections in spite of a larger settling velocity of CSM. The southward sediment flux at the cross section N on 15 January was calculated to be $10.5\,\mathrm{t\,s^{-1}}$ for FSM and $9.3\,\mathrm{t\,s^{-1}}$ for CSM when the wave effect was not considered (Expt. 1 in Table 1). In comparison, the sediment flux at the cross section S was computed to be 7.1 and $4.3\,\mathrm{t\,s^{-1}}$ for FSM and CSM, respectively.

When the wave forcing was included in the model experiment, the model predicted southward flux at the cross section N was increased to $25.6\,\mathrm{t\,s^{-1}}$ for FSM and $24.1\,\mathrm{t\,s^{-1}}$ for CSM, respectively (Expt. 2 in Table 1). This increase was caused by the

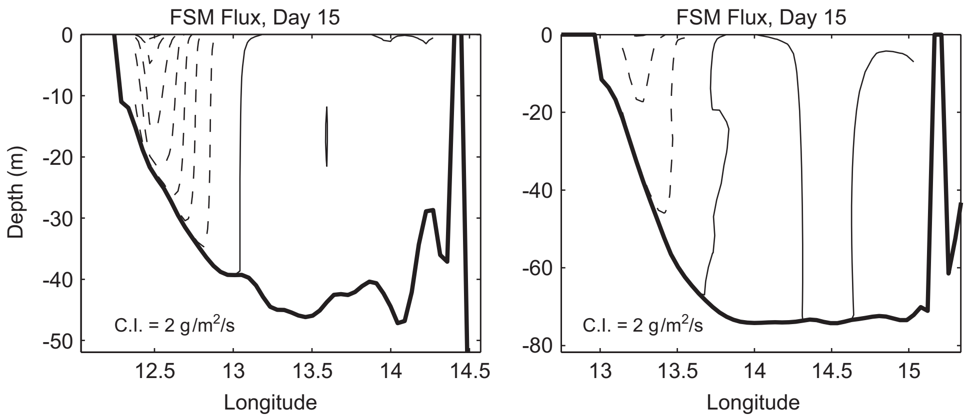

Fig. 11. Model simulated horizontal FSM fluxes at cross section N (left) and cross section S (right) on 15 January 2001, by Experiment 1.

increased sediment concentration in the water column over the western shelf despite a decrease in the southward alongshore current (by up to 6 cm s^{-1} near the bottom). Similarly, the southward flux for FSM and CSM at cross section S was also increased by 50% and 84%, respectively (Table 1).

3.4. Effect of wave and current alignment

In order to verify the importance of the angle (θ) between the wave and current in determining the maximum bottom stress calculated by (2), Experiment 2 was repeated by assuming the wave direction and bottom current velocity was aligned (Experiment 3). The model results showed that the bottom stress was only slightly larger than that predicted by Experiment 2 during the Bora event (Fig. 5). With respect to Experiment 2, Experiment 3 overpredicted the sediment flux by 8% (FSM) and 9% (CSM) at the cross section N, but produced negligible difference at the cross section S (Expt. 3 in Table 1). These small difference between the two experiments demonstrated that the sediment transport model was insensitive to the angle between directions of the wave propagation and current in the NAS where large waves were generated by the Bora storm, as already shown by Grant and Madsen (1979) for strong wave conditions.

3.5. Effect of tides on southward sediment flux

To examine the effect of tides on the sediment resuspension and southward flux, the AIM open boundary conditions need to be modified to include tidal forcing in the model.

We first conducted a tide only model run with appropriate nodal correction so that the model time was matched with the calendar year. However, in order to verify the model results with known amplitudes and phases of 15 Adriatic ports (i.e. ports of Otranto, Brindisi, Manfredonia, Vieste, Ortona, Ancona, Pesaro, Ravenna, Venezia, Trieste, Rovinj, Dubrovnik, Bar, Durres and Palagruža) the model run was applied for homogeneous temperature (= 13 °C) and salinity field (= 38). The model run lasted over the first 270 days of a year. After 80 days of the spin-up period hourly values of sea-surface elevation of the remaining 190 days were analysed. The Rayleigh criterion for the separation of seven major constituents was therefore fully respected (the synodic period for the separation of S_2 and K_2 is 182.6 days). Along the open boundary, the amplitudes and phases of tidal elevation were interpolated from the known data of nearby ports of South Adriatic, Italy and Greece for the seven principal tidal constituents M_2, K_2, S_2, N_2, K_1, P_1 and O_1. After the tidal model run with these open boundary conditions, the trigonometric fit of the amplitudes and phases of 15 Adriatic ports was performed. The difference between modelled and observed amplitudes and phases in the port of Trieste was used for the calibration of the open boundary conditions. This procedure was iteratively repeated four times to obtain the satisfying results of tidal amplitudes at the 15 ports that had a maximum error less than 2.2, 1.5, 1.6, 1.1, 2.1, 1.7 and 0.7 cm for M_2, K_2, N_2, S_2, K_1, P_1 and O_1, respectively (Table 3). Two- and three-dimensional (total) velocities at the open boundary were saved at every time step to the files and then used in the successive run as velocity boundary conditions without elevation. The least square analysis of the elevations in 15 ports of both runs (those with elevation boundary conditions, and those with velocity boundary conditions) did not show any significant difference. These velocities were then included in the open boundary conditions of the general circulation model (AIM) for tidal forcing. The CFL criterion is fulfilled with the external time step of AIM (7 s), since the maximum modeled depth is 2700 m and the barotropic signal passes the grid-cells of 5 km in time interval larger than 30 s. The tidal model internal time step is also the same as that of AIM (700 s).

As shown in Fig. 12, when the tidal forcing was included in the AIM with the effect of waves (Expt. 4), the hydrodynamics of the BBL properties, bed load and sediment concentration was not significantly altered. In response to the tidal forcing, the value of bottom current speed, stress and CSM concentration was slightly modified with some fluctuation at a semi-diurnal frequency. As the tidal current shear was much weaker than that of wind driven current during the Bora event, the contribution of the tides to the vertical mixing was negligible in the water column (figure not shown). The model predicted total southward flux at the cross section N and S was reduced by 1% and 21%, respectively, when compared with that predicted by Experiment 2 (Expt. 4 in Table 1). The decreased flux coincided with northward tidal current at the time of flux computation. The northward tidal current had reduced the southward alongshore mean current on the western shelf. At the cross section S, the tidal current was stronger resulting in a larger reduction in the southward sediment flux. It should be noted that at a phase when the tidal current directions were reversed in the NAS, the sediment flux was predicted to be slightly increased by similar proportions at both cross-sections.

3.6. *Effect of sediment-induced stratification on the southward sediment flux*

In this study we have assumed that the sediments had no contribution to the water density, therefore the water stratification was not affected by the resuspended sediments. To validate this assumption, Experiment 2 was repeated with a new parameterization of the bottom drag coefficient that

Table 3
Modelled (Z_m), observed (Z_o) amplitudes and their absolute difference for each of seven major constituents in 15 ports along the Adriatic coastline, where the ports of Otranto, Brindisi, Manfredonia, Vieste, Ortona, Ancona, Pesaro, Ravenna, Venezia, Trieste, Rovinj, Dubrovnik, Bar, Durres and Palagruža and Split are denoted with only first three letters of their names

		OTR	BRI	MAN	VIE	ORT	ANC	PES	RAV	VEN	TRI	ROV	DUB	BAR	DUR	PAL	< >	Max
M_2	Z_o	6.5	8.7	10.0	7.9	6.4	6.0	12.8	15.5	23.4	26.7	19.3	8.7	9.2	9.3	10.0		
	Z_m	8.1	9.5	10.4	9.4	5.5	6.8	12.7	17.7	24.0	26.7	19.6	9.9	10.0	9.8	8.3		
	$\|Z_o\text{-}Z_m\|$	1.6	0.8	0.4	1.5	0.9	0.8	0.1	2.2	0.6	0.0	0.3	1.2	0.8	0.5	1.7	0.9	2.2
K_2	Z_o	1.7	1.4	2.7	1.9	2.1	0.2	1.8	2.5	5.3	4.3	3.0	2.1	1.7	1.5	3.0		
	Z_m	1.3	1.6	1.8	1.7	1.1	1.0	2.1	2.9	4.1	4.6	3.3	1.7	1.7	1.7	1.5		
	$\|Z_o\text{-}Z_m\|$	0.4	0.2	0.9	0.2	1.0	0.8	0.3	0.4	1.2	0.3	0.3	0.4	0.0	0.2	1.5	0.5	1.5
N_2	Z_o	1.2	1.4	1.6	1.9	0.9	1.3	3.2	3.0	3.8	4.5	3.5	1.5	1.3	0.6	3.0		
	Z_m	1.4	1.6	1.8	1.6	0.8	1.3	2.3	3.1	4.2	4.6	3.4	1.7	1.7	1.7	1.4		
	$\|Z_o\text{-}Z_m\|$	0.2	0.2	0.2	0.3	0.1	0.0	0.9	0.1	0.4	0.1	0.1	0.2	0.4	1.1	1.6	0.4	1.6
S_2	Z_o	4.0	5.2	6.1	5.1	4.5	3.2	6.8	9.1	13.8	16.0	11.2	5.8	5.6	5.5	5.9		
	Z_m	4.5	5.6	6.3	5.8	3.9	3.5	7.1	10.2	14.2	16.0	11.5	6.0	6.0	5.9	5.3		
	$\|Z_o\text{-}Z_m\|$	0.5	0.4	0.2	0.7	0.6	0.3	0.3	1.1	0.4	0.0	0.3	0.2	0.4	0.4	0.6	0.4	1.1
K_1	Z_o	2.5	4.6	4.7	4.2	9.7	12.8	15.4	15.9	16.0	18.2	16.1	5.5	4.8	5.0	6.0		
	Z_m	4.3	5.9	5.8	6.3	10.1	13.6	15.3	16.4	17.7	18.1	16.8	6.4	6.3	6.2	7.9		
	$\|Z_o\text{-}Z_m\|$	1.8	1.3	1.1	2.1	0.4	0.8	0.1	0.5	1.7	0.1	0.7	0.9	1.5	1.2	1.9	1.1	2.1
P_1	Z_o	0.8	1.5	1.7	1.5	3.0	4.1	4.2	5.3	4.3	6.0	5.3	1.6	1.4	1.4	3.0		
	Z_m	1.5	2.0	1.9	2.1	3.4	4.5	5.1	5.5	6.0	6.1	5.6	2.2	2.1	2.1	2.6		
	$\|Z_o\text{-}Z_m\|$	0.7	0.5	0.2	0.6	0.4	0.4	0.9	0.2	1.7	0.1	0.3	0.6	0.7	0.7	0.4	0.6	1.7
O_1	Z_o	1.1	1.5	1.7	1.6	3.4	4.0	5.1	5.0	5.2	5.4	4.9	2.1	1.9	1.6	3.0		
	Z_m	1.8	2.2	2.1	2.2	3.3	4.2	4.7	5.0	5.3	5.4	5.1	2.4	2.3	2.3	2.7		
	$\|Z_o\text{-}Z_m\|$	0.7	0.7	0.4	0.6	0.1	0.2	0.4	0.0	0.1	0.0	0.2	0.3	0.4	0.7	0.3	0.3	0.7

The average ⟨ ⟩ and maximum value were calculated out from 15 ports.

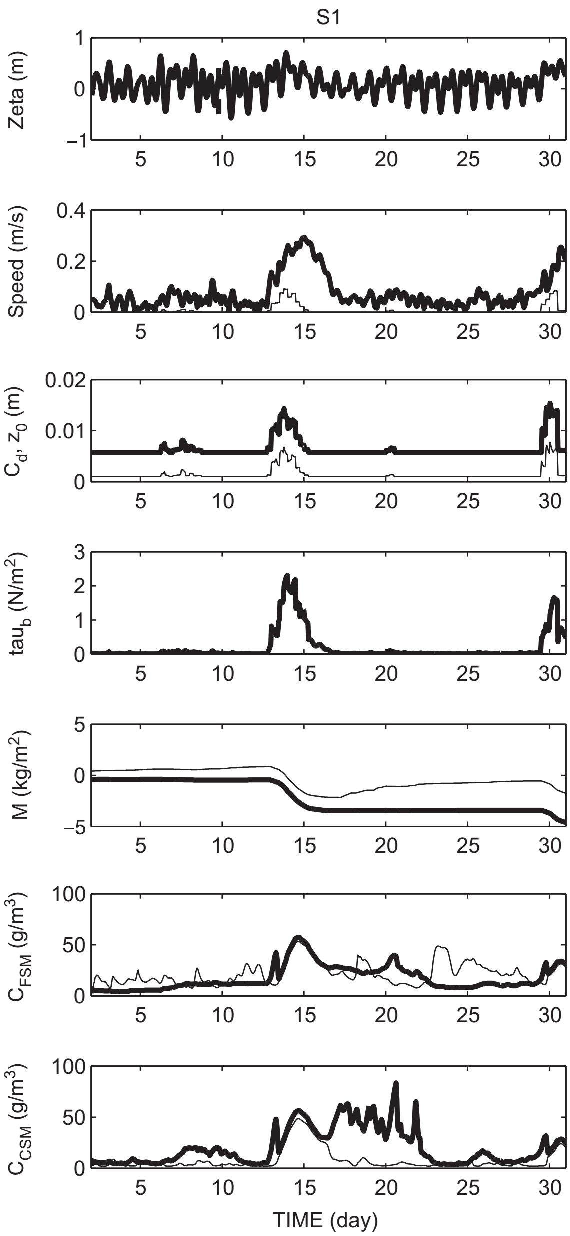

Fig. 12. The same as Fig. 5 but predicted by Experiment 4. The surface elevation at S1 is also shown in the top panel.

considered the sediment-induced stratification in the BBL (Wang, 2002):

$$C_d = \left[\frac{1}{\kappa/(1+AR_f)}\ln(H+z_b)/z_0\right]^{-2}, \tag{7}$$

where A (= 5.5) is an empirical constant and R_f is a flux Richardson number computed by the Mellor–Yamada turbulent closure scheme. The sediment concentration and the water density were also coupled by a simple bulk density relation (Wang, 2002).

Due to low sediment concentration in the study region, the sediment-induced stratification had negligible effect on the sediment flux at both cross sections (Expt. 5, Table 1). The sediment fluxes were changed by less than 1% for both FSM and CSM (Table 1).

4. Discussion and conclusions

The Adriatic Sea general circulation model (AIM) coupled to a sediment transport model with and without the effect of the waves simulated by SWAN was implemented in the Adriatic Sea to study the dynamics of the sediment transport and resuspension in the NAS during the Bora event in January 2001, when large currents and waves were generated by strong winds. The general features of model predicted WACC and wave fields agreed with the observations on the western Adriatic shelf. The BBL was resolved by the coupled model with high vertical resolution, and the effect of the wave–current interaction on the bottom stress was represented in the model. By including the tidal forcing in the coupled model, we also examined the effect of tides on the sediment transport dynamics in the NAS.

The study found that, during the Bora event of 13–17 January 2001, waves with significant wave height and period of 2 m and 5 s, respectively, were generated by the strong winds in the NAS. The wave–current interaction in the BBL increased the bottom stress over the western Adriatic shelf, resulting in strong sediment resuspension there. Combining large coastal currents and upward turbulence-driven vertical flux of resuspended sediments, the model predicted total significantly larger southward sediment flux at the cross section N than the prediction by the model run excluding wave forcing. The model predicted southward fluxes at the cross section S were much smaller than those predicted at cross section N, as the waves had less effect on sediment resuspension there. Inclusion of the waves in the model forcing increased the total sediment flux at that cross section.

It should be noted that large southward sediment fluxes shown above were clearly maintained by two important processes: a vigorous vertical mixing in the water column and a strong bottom sediment resuspension. The former was a combination of wind and convective cooling mixing during the Bora event. The latter was enhanced by the combined motion of the wave and current in the BBL in the manner discussed previously. As correctly pointed out by a reviewer, wave–current coupling can also enhance mixing in the surface boundary layer where breaking of waves frequently occurs (e.g., Craig and Banner, 1994; Terray et al., 1996). Although this mechanism was not included in the current study, its effect on sediment distribution and fluxes in the NAS should not be significant to change our conclusion for the reason that the water column was already well mixed due to strong current shear driven by the Bora winds and shallow water depth there (Fig. 5).

It should be further noted that southward fluxes were much weaker along the western coast south of Ancona (Fig. 10). The model predicted sediment plumes were only confined to the western Adriatic shelf north of Ancona (Fig. 7a). Fig. 13 shows monthly net sedimentation simulated by the Experiments 1 and 2. Two CSM depocentres are found with one location adjacent to Po Prodelta and the other near Ancona Promontory. We note that no net FSM sedimentation was predicted in the NAS and that deposition/erosion patterns predicted by the Experiment 1 are similar to that from Experiment 2 but with smaller rates. No significant difference was found between predictions between Experiments 2 and 4 (figure not shown). In comparison with Holocene sedimentation shown in Fig. 1a, several conclusions can be drawn for the sediment transport in the NAS.

Firstly, the depocentre near Ancona is largely attributed to CSM accumulation and the sediment source is the Po River discharge as well as erosion along a coastal band from the Po to the north of Ancona. Moreover, both sedimentation and erosion rate in these areas was doubled due to the combined motion of wave–current in the BBL during the Bora event. Given that the NAS experiences frequent Bora storms (8–10 events) in winter seasons (Wang et al., 2006), the sediment transport driven by waves and currents during these Bora events may be a significant mechanism for long term NAS sediment deposition in the area near Ancona as depicted by the Holocenic sedimentation (Fig. 1a). As expected, the model results showed no net effect of tides on sedimentation anywhere in the NAS. Furthermore, based on the model predicted sedimentation in the depocentre near Po River mouth and a bulk density value of $1500\,\mathrm{kg\,m^{-3}}$ (Wheatcroft et al., 2006), the annual sedimentation rate is about $3.3\,\mathrm{cm\,yr^{-1}}$ (if 10 Bora events per year was used). This value agrees well with the rate found by Palinkas et al. (2005), which is $2–6\,\mathrm{cm\,yr^{-1}}$ (Table 2).

In order to test the model sensitivity to settling velocity, we repeated Experiment 2 by using $w_s = -10^{-3}\,\mathrm{m\,s^{-1}}$ that represents a floc settling rate found by Fox et al. (2004b) in the NAS. Fig. 13c shows the model predicted monthly floc sedimentation. The locations of both depocentres predicted by Experiment 2 remained unchanged. However, it is clear that flocculation of fine sediments in the NAS has reduced erosion and increased sedimentation rates, respectively, along the shallow Italian coastal region north of Ancona.

Secondly, relatively high sediment concentrations along the western coastal region south of Ancona were clearly locally driven by the wave resuspension events (Fig. 7b). While the winter phytoplankton bloom of the northwestern Adriatic shelf is primarily supported by the high nutrient run-off from the Po River (Zavatarelli et al., 2000), locally driven bottom resuspension may play a dominant role in supplying benthic nutrients and remineralized refractory organic matters to sustain the often observed high primary production in the coastal region further south of Ancona (e.g. Zavatarelli et al., 2000). Giordani et al. (1992) pointed out that this mechanism is a significant source of nutrients in the NAS.

From this work we presented modelling predictions of sediment transport processes in the NAS during a winter Bora event. The numerical study demonstrated that wave–current interaction in the BBL enhanced the bottom stress and therefore greatly increased the sediment resuspension concentrations in the water column. The study also demonstrated that the enhanced bottom stress due to wave–current interaction was insensitive to the angle between the directions of wave propagation and bottom currents. These results signified wave effect on sediment flux and distribution in the NAS. Finally, we have shown that tides caused negligible change in the sediment transport at the cross section N, but with some minor fluctuation in the sediment fluxes within a tidal period at cross section S.

Due to lack of observation for model data comparison, this study is of an exploratory nature and the conclusions are preliminary. Since the bottom sediment resuspension controls the pelagic and benthic biogeochemical processes such as

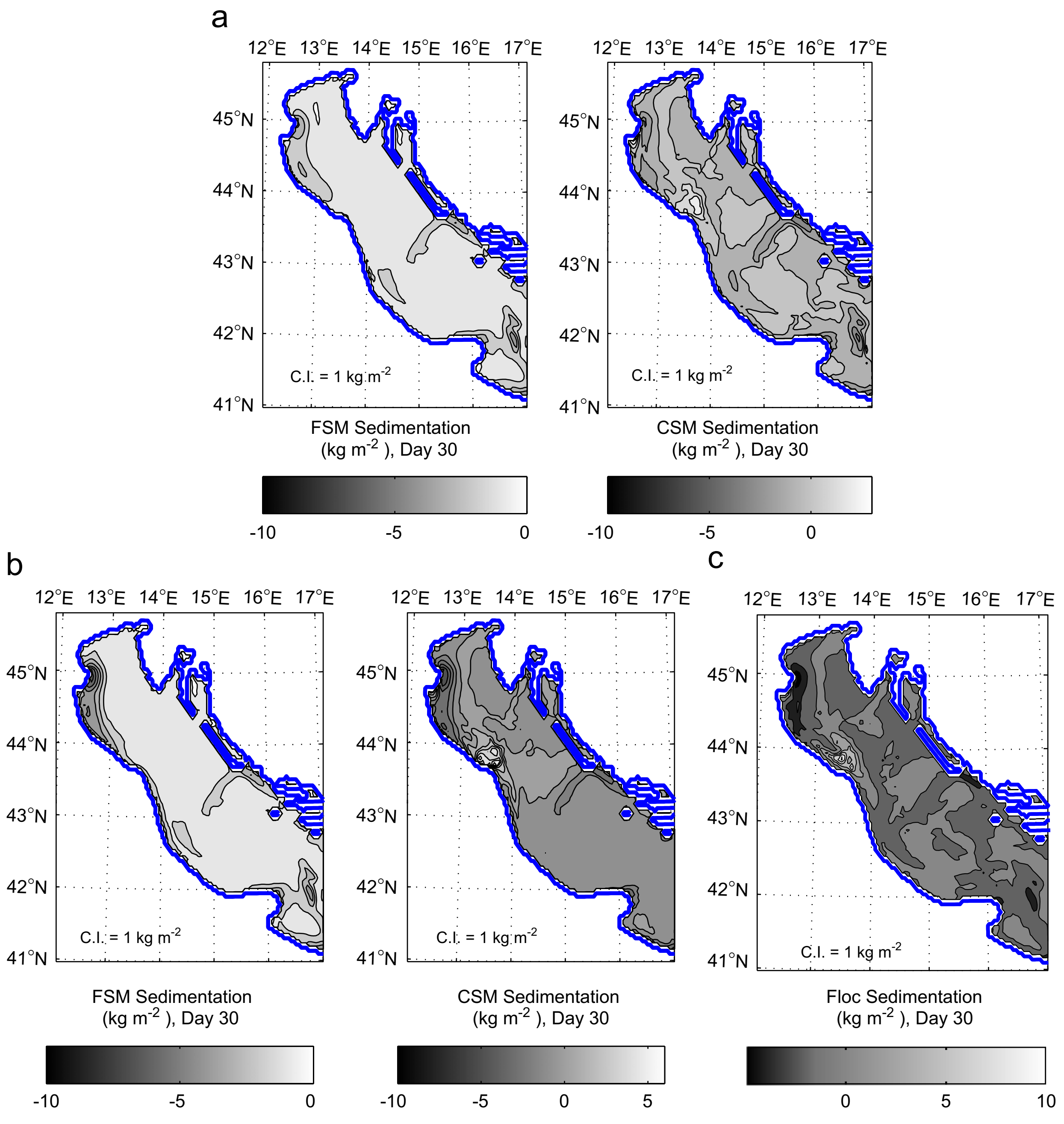

Fig. 13. Model simulated monthly net sedimentation by (a) Experiment 1; (b) Experiment 2, and (c) Experiment 2, but $w_s = -10^{-3}\,\mathrm{m\,s^{-1}}$.

photosyntheticly active radiance attenuation by suspended sediments and the microbial remineralization of suspended refractory organic matters from the benthic system, inclusion of a wave–current coupled sediment transport model in the future ecosystem models may result in a more accurate representation of the primary production in the turbid coastal environments such as the NAS.

Acknowledgments

The Adriatic Intermediate Model was developed by Dr. M. Zavatarelli and Dr. Paolo Oddo in the ADRICOSM project. We thank to Mr. B. Petelin for his assistance in building the Adriatic Sea tidal model. X.H. Wang was supported by the 2002 UNSW John Yu Fellowship to Europe and the

Italian Ministry for Environment and Territory through the ADRICOSM project. Prof. N. Pinardi was supported by the ADRICOSM project. The wave data were provided by Envirtech (http://www/envirtech.org/ron.asp). Dr. J. Wei's assistance in figure preparation is also acknowledged. An APAC-MAS grant was received for the numerical computations for this work. Discussion with Prof. O. S. Madsen and Dr. T. T.-J. Hsu and the editorial assistance from Ms. Julie Kesby improved the paper.

References

Ariathurai, R., Krone, R.B., 1976. Mathematical modelling of sediment transport in estuaries. In: Wiley, M. (Ed.), Estuarine Processes, vol. II. Academic Press, New York, pp. 98–106.

Artegiani, A., Bregant, D., Paschini, E., Pinardi, N., Raicich, F., Russo, A., 1997a. The Adriatic Sea general circulation. Part I: Air–sea interactions and water mass structure. Journal of Physical Oceanography 27, 1492–1514.

Artegiani, A., Bregant, D., Paschini, E., Pinardi, N., Raicich, F., Russo, A., 1997b. The Adriatic Sea general circulation. Part II: Baroclinic circulation structure. Journal of Physical Oceanography 27, 1515–1532.

Blumberg, A.F., Mellor, G.L., 1987. A description of a three-dimensional coastal ocean circulation model. In: Nihoul, J.C.J., Jamart, B.M. (Eds.), Three-dimensional Models of Marine and Estuarine Dynamics. Elsevier Oceanography Series, vol. 45, Amsterdam, pp. 55–88.

Boldrin, A., Langone, L., Miserocchi, S., Turchetto, M., Acri, F., 2005. Po River plume on the Adriatic continental shelf: dispersion and sedimentation of dissolved and suspended matter during different river discharge rates. Marine Geology 222–223, 135–158.

Booij, N., Ris, R.C., Holthuijsen, L.H., 1999. A third-generation wave model for coastal regions. Part I—Model description and validation. Journal of Geophysical Research 104, 7649–7666.

Brambati, A., Bregant, D., Lenardon, G., Stolfa, D., 1973. Transport and Sedimentation in the Adriatic Sea. Pubblicazione N. 20 del Museo Friulano di Storia Naturale, 60pp.

Byun, D.S., Wang, X.H., 2005. Numerical studies on the dynamics of tide and sediment transport in the western tip of the southwest coast, Korea. Journal of Geophysical Research 110 (C03011).

Cavaleri, L., Bertotti, L., 1997. In search of the correct wind and wave fields in a minor basin. Monthly Weather Review 125, 1964–1975.

Cavaleri, L., Curiotto, S., Mazzoldi, A., Pavanati, M., 1997. Long term directional wave recording in the Northern Adriatic Sea. Il Nouvo Cimento 20, 103–110.

Clarke, S., Elliott, A.J., 1998. Modelling suspended sediment concentration in the Firth of Forth. Estuarine, Coastal and Shelf Science 47, 235–250.

Correggiari, A., Trincardi, F., Langone, L., Roveri, M., 2001. Styles of failure in heavily-sedimented highstand prodelta wedges on the Adiatic shelf. Journal of Sedimentary Research 71, 218–236.

Craig, P.D., Banner, M.L., 1994. Modeling wave-enhanced turbulence in the ocean surface layer. Journal of Physical Oceanography 24, 2513–2529.

Eidsvik, K.J., 1993. Parameterization of wave effects upon large-scale bottom boundary layer flow. Continental Shelf Research 13, 903–918.

Fox, J.M., Hill, P.S., Milligan, T.G., Boldrin, A., 2004a. Flocculation and sedimentation on the Po River Delta. Marine Geology 203, 95–107.

Fox, J.M., Hill, P.S., Milligan, T.G., Ogston, A.S., Boldrin, A., 2004b. Floc fraction in the waters of the Po River prodelta. Continental Shelf Research 24, 1699–1715.

Frascari, F., Frignani, M., Guerzoni, S., Ravaioli, M., 1988. Sediments and pollution in the Northern Adriatic Sea. Annals of the New York Academy of Sciences 534, 1000–1020.

Giordani, P., Hammond, D.E., Berelson, W.M., Montanari, G., Poletti, R., Milandri, A., Frignani, M., Langone, L., Ravailoi, M., Rovatti, G., Rabbi, E., 1992. Benthic fluxes and nutrient budgets for sediments in the Northern Adriatic Sea: burial and recycling efficiencies. Science of the total Environment, Supplement, 251–275.

Grant, W.D., Madsen, O.S., 1979. Combined wave and current interaction with a rough bottom. Journal of Geophysical Research 84, 1797–1808.

Holthuijsen, L.H., Booij, N., Herbers, T.H.C., 1989. A prediction model for stationary, short-crested waves in shallow water with ambient currents. Coastal Engineering 13, 23–54.

Khan, S.M., Imran, J., Bradford, S., Syvitski, J., 2005. Numerical modeling of hyperpycnal plume. Marine Geology 222–223, 193–211.

Kourafalou, V.H., 1999. Process studies on the Po River plume, North Adriatic Sea. Journal of Geophysical Research 104, 29,963–29,985.

Lee, C.M., Askari, F., Brook, J., Carniel, S., Cushman-Rosin, B., Dorman, C., Doyle, J., Flament, P., Harris, C.K., Jones, B.H., Kuzmic, M., Martin, P., Ogston, A., Orlic, M., Perkins, H., Poulain, P.-M., Pullen, J., Russo, A., Sherwood, C., Signell, R.P., Thaler Detweiler, D., 2005. Northern Adriatic response to a wintertime Bora wind event. EOS Transactions 86 (16), 19.

Madsen, O.S., Poon, Y.-K., Graber, H.C., 1988. Spectral wave attenuation by bottom friction: theory. In: Proceedings of the 21th International Conference on Coastal Engineering, ASCE, New York, pp. 492-504.

Maggiore, A., Zavatarelli, M., Angelucci, M.G., Pinardi, N., 1998. Surface heat and water fluxes in the Adriatic Sea: seasonal and interannual variability. Physical Chemical and Earth Sciences 23 (5-6), 561–567.

Malacic, V., Viezzoli, D., Cushman-Roisin, B., 2000. Tidal dynamics in the northern Adriatic Sea. Journal of Geophysical Research 105, 26,265–26,280.

Malanotte-Rizzoli, P., Bergamasco, A., 1983. The dynamics of the coastal regions of the Northern Adriatic Sea. Journal of Physical Oceanography 13, 1105–1130.

Matteucci, G., Frascari, F., 1997. Fluxes of suspended materials in the north Adriatic Sea (Po Prodelta area). Water, Air and Soil Pollution 99, 557–572.

Mellor, G.L., Wang, X.H., 1996. Pressure compensation and the bottom boundary layer. Journal of Physical Oceanography 26, 2214–2222.

Mikkelsen, O.A., Hill, P.S., Milligan, T.G., Chant, R.J., 2005. In situ particle size distributions and volume concentrations from a LISST-100 laser particle sizer and a digital floc camera. Continental Shelf Research 25, 1959–1978.

Nittrouer, C., Miserocchi, S., Trincardi, F., 2004. The PASTA project: investigation of Po and Apenine sediment transport and accumulation. Oceanography 17 (4), 46–57.

Palinkas, C.M., Nittrouer, C.A., Wheatcroft, R.A., Langone, L., 2005. The use 7Be to identify event and seasonal sedimentation near the Po River delta, Adriatic Sea. Marine Geology 222–223, 95–112.

Poulain, P.-M., 2001. Adriatic Sea surface circulation as derived from drifter data between 1990 and 1999. Journal of Marine System 29, 3–32.

Pullen, J., Doyle, J.D., Hodur, R., Ogston, A., Book, J.W., Perkins, H., Signell, R., 2003. Coupled ocean–atmosphere nested modeling of the Adriatic Sea during winter and spring 2001. Journal of Geophysical Research 108, C103320.

Raicich, F., 1996. On the fresh water balance of the Adriatic Sea. Journal of Marine System 9, 305–319.

Ravaioli, M., Alvisi, F., Vitturi, L.M., 2003. Dolomite as a tracer for sediment transport and deposition on the northwestern Adriatic continental shelf (Adriatic Sea, Italy). Continental Shelf Research 23, 1359–1377.

Ris, R.C., Booij, N., Holthuijsen, L.H., 1999. A third-generation wave model for coastal regions. Part II—Verification. Journal of Geophysical Research 104, 7667–7681.

Sherwood, C.R., Book, J., Carniel, S., Cavaleri, L., Chiggiato, J., Das, H., Doyle, J.D., Harris, C.K., Niedoroda, A.W., Perkins, H., Poulain, P.-M., Pullen, J., Reed, C.W., Russo, A., Sclavo, M., Signell, R.P., Traykovski, P., Warner, J.C., 2004. Sediment dynamics in the Adriatic Sea investigated with coupled models. Oceanography 17 (4), 58–69.

Signell, R.P., Carniel, S., Cavaleri, L., Chiggiato, J., Doyle, J., Pullen, J., Sclavo, M., 2005. Assessment of operational wind models for the Adriatic Sea using wind and wave observations: a first analysis focused on the Venice lagoon region. Journal of Marine System 53, 217–233.

Smagorinsky, J., 1963. General circulation experiments with the primitive equations, I: The basic experiment. Monthly Weather Review 91, 99–164.

Smorlarkiewicz, P.K., 1984. A fully multidimensional positive definite advection transport algorithm with small implicit diffusion. Journal of Computational Physics 54, 325–362.

Terray, E.A., Donelan, M.A., Agrawal, Y.C., Drennan, W.M., Kahma, K.K., Williams III, A.J., Hwang, P.A., Kitaigorodskii, S.A., 1996. Estimates of kinetic energy dissipation under breaking waves. Journal of Physical Oceanography 26, 792–807.

Traykovski, P., Wiberg, P.L., Geyer, W.R., 2006. Observations and modeling of wave-supported sediment gravity flows on the Po prodelta and comparison to prior observations from the Eel shelf. Continental Shelf Research, 111, C03S17, doi:10.1029/2005JC003110.

Wang, X.H., 2001. A numerical study of sediment transport in a coastal embayment during a winter storm. Journal of Coastal Research 34 (Special Issue), 414–427.

Wang, X.H., 2002. Tide-induced sediment resuspension and the bottom boundary layer in an idealized estuary with a muddy bed. Journal of Physical Oceanography 32, 3113–3131.

Wang, X.H., Pinardi, N., 2002. Modeling the dynamics of sediment transport and resuspension in the Northern Adriatic Sea. Journal of Geophysical Research 107 (C12).

Wang, X.H., 2005. Circulation of the northern Adriatic Sea (Italy) due to a Bora event in January 2001: a numerical model study. Ocean Modeling 10, 253–271.

Wang, X.H., Oddo, P., Pinardi, N., 2006. On the bottom density plume on coastal zone off Gargano (Italy) in the southern Adriatic Sea and its inter-annual variability. Journal of Geophysical Research 111, C03S17, doi:10.1029/2005JC003110.

Warren, R., Johnsen, J., 1993. Cohesive sediment modelling for coastal lagoons. In: The Proceedings of the International Colloquium and Exposition on Computer Applications in Coastal and Offshore Engineering (ICE-CACOE'93), Kuala Lumper, Malaysia, June 14–16, 1993.

Wheatcroft, R.A., Stevens, A.W., Hunt, L.M., Milligan, T.G., 2006. The large-scale distribution and internal geometry of the fall 2000 Po River flood deposit: evidence from digital x-radiography. Continental Shelf Research 26, 499–516.

Zavatarelli, M., Baretta, J.W., Baretta-Bekker, J.G., Pinardi, N., 2000. The dynamics of the Adriatic Sea ecosystem. An idealized model study. Deep-Sea Research I 47, 937–970.

Zavatarelli, Z., Pinardi, N., Kourafalou, V.H., Maggiore, A., 2002. Diagnostic and prognostic model studies of the Adriatic Sea general circulation. Part I: The seasonal variability. Journal of Geophysical Research 107, 3004.

Zavatarelli, M., Pinardi, N., 2003. The Adriatic Sea modelling system: a nested approach. Annales Geophysicae 21, 345–364.